Auger recombination in semiconductor quantum wells in a magnetic field

Georgii G. Samsonidze and Georgy G. Zegrya
A. F. Ioffe Physico-Technical Institute, 26 Polytekhnicheskaya, St. Petersburg 194021, Russia
(Received 24 July 2000; published 1 February 2001)

Auger process involving two electrons from the conduction band and a heavy hole from the valence band in semiconductor heterostructures with quantum wells is investigated for the case of a magnetic field applied normal to heteroboundaries. It is shown that there exist three different mechanisms of Auger recombination, associated with (I) electron scattering at interface with transition into the continuous spectrum, (II) short-range Coulomb interaction in the quantum well with transition into the continuous spectrum, and (III) resonance transition into the discrete spectrum. All these processes are thresholdless. The Auger recombination coefficients analytically calculated for the processes I, II, and III show different dependencies on temperature, magnetic field, and quantum well parameters. In the limit of an infinitely wide quantum well, processes I and II merge to form a bulk threshold Auger process, while process III remains thresholdless resonance one. In the limit of infinitely weak magnetic field, process I remains thresholdless, process II becomes a quasithreshold process (i.e., its threshold energy slightly depends on temperature), and process III transforms into a nonresonance process with a threshold. The results obtained are new and have no analogies in the literature.

DOI: 10.1103/PhysRevB.63.075317 PACS number(s): 73.40.−c, 71.20.Mq, 75.50.Pp, 78.66.Hf

I. INTRODUCTION

The Auger process is one of the most important mechanisms of nonradiative charge carrier recombination in semiconductors. Various Auger recombination channels in homogeneous semiconductors have long been investigated in the absence of magnetic field.[1–3] Two Auger recombination processes, the first involving two electrons and a heavy hole (CHCC Auger process), and the second involving an electron and two heavy holes (CHHS Auger process), take place in narrow-gap semiconductors.[2] It has been shown that the rate of Auger recombination depends on temperature exponentially, i.e., Auger recombination processes are characterized by a threshold.[2] In an Auger recombination event, the third (excited) particle acquires, owing to the Coulomb interaction, a large amount of energy on the order of the gap width E_g. Therefore, the excited particle must also acquire a large momentum. By virtue of the momentum conservation law the system of interacting electrons and holes must also possess a large momentum, and consequently high energy, before recombination. Therefore, only those particles can participate in recombination whose total kinetic energy is sufficiently high (much higher than the average kinetic energy of particles). This means that Auger recombination has an energy threshold. However, the presence of magnetic field removes the threshold for the transitions to the discrete spectrum (to high-excited Landau levels) in homogeneous semiconductors.[4]

The disappearance of the threshold can be explained qualitatively. The electron spectrum is discrete in the direction perpendicular to the magnetic field. An Auger electron with energy approximately equal to the gap width makes vertical transition to a high Landau level without quasimomentum change as a result of Coulomb interaction. Therefore, it is not required a large quasimomentum to be transferred in a Coulomb interaction of two electrons. It is only necessary that the Auger electron be delivered exactly to the Landau level. Therefore, the Auger process is resonant in a quantizing magnetic field. Hence, the Auger process rate oscillates as a function of the magnetic field strength.

An Auger process involving a transition to a light hole state has been investigated in terms of three-band Kane's model in bulk semiconductors, and oscillations of the transition rate as a function of magnetic field strength have been observed.[4] Auger transitions in quantum wells in strong magnetic fields have been detected in luminescence[5] and cyclotron resonance[6] experiments. Both these papers notice the resonance behavior of the Auger process probability as a function of magnetic field. The Auger process rate in a quantum well with magnetic field has also been calculated.[7] However, the real band structure of semiconductors has been neglected and only interband transitions between electron Landau levels have been taken into account. The rates of Auger processes in semiconductors with complicated valence band structure (i.e., with heavy hole states taken into account) in a magnetic field have not been reported in the literature.

It is commonly assumed that the reasons for Auger recombination in quantum wells are the same as in homogeneous semiconductors.[8,9] Nevertheless, the threshold disappears in a quantum well for a transition to the discrete spectrum even without any magnetic field.[10–12] The presence of heteroboundaries removes the limitations imposed on the electron–electron interaction processes by the energy and momentum conservation principles, since the excited Auger electron acquires necessary quasimomentum when interacting with (being scattered at) the heteroboundary. Namely, the conservation of the momentum component normal to the heteroboundary surface is removed with new thresholdless Auger recombination channels formed in heterostructures. All of them have been investigated repeatedly. In particular, threshold and thresholdless Auger recombination channels have been analyzed for a single heteroboundary.[10] The thresholdless Auger recombination channel correlated with small momenta transferred in Coulomb interaction of particles has been studied.[11] The threshold and thresholdless

Auger recombination channels in quantum wells, corresponding to electron scattering at heteroboundaries and to Coulomb electron scattering in the quantum well volume, have been calculated.[12]

The purpose of this work is to investigate theoretically the basic Auger recombination channels in a semiconductor quantum well with perpendicularly applied magnetic field. The Auger process involving two electrons from the conduction band and a heavy hole from the valence band (CHCC Auger process) is studied. In this process, the first electron recombines with the heavy hole, and the second proceeds to high excited state as a result of the Coulomb interaction. This state may lie in a continuous or discrete energy spectrum. There are three fundamentally different Auger recombination channels based on (1) electron scattering at the heteroboundary and transition to a continuous spectrum state, (2) Coulomb electron scattering in the volume of the quantum well and transition to a continuous spectrum state, and (3) resonance transition to a discrete spectrum state. It is shown that the rates of the Auger recombination processes corresponding to different channels have different dependencies on temperature, magnetic field strength, and quantum well parameters. The paper is organized in the following way. In Sec. II, a brief description of the wave functions and the energy spectra of electrons and holes is given. In Sec. III, the Auger recombination coefficients are calculated. In Sec. IV, the results are analyzed and discussed. The summarizing remarks follow in Sec. V.

II. SPECTRA AND WAVE FUNCTIONS OF CHARGE CARRIERS

Wave functions of charge carriers are to be known for analyzing the Auger recombination mechanism and calculating the Auger process rate. Wave functions are to be found using a multiband approximation, as it has been done for bulk Auger processes.[2] We use four-band Kane's model describing the wave functions and energy spectrum of carriers in narrow-gap $A_{III}B_V$ semiconductors with the highest precision.[13] Usually the eigenfunctions of the angular momentum are taken as basis functions of the conduction and valence bands.[13,14] However, we choose the representation of the basis functions

$$|S\uparrow\rangle,|S\downarrow\rangle,|X\uparrow\rangle,|X\downarrow\rangle,|Y\uparrow\rangle,|Y\downarrow\rangle,|Z\uparrow\rangle,|Z\downarrow\rangle, \tag{1}$$

more useful for our purposes, where $|S\rangle$, $|X\rangle$, $|Y\rangle$, and $|Z\rangle$ are the Bloch functions of the S and P type with angular momenta of 0 and 1, respectively. The first of them describes the conduction band state, and the others the valence band state at the center of the Brillouin zone. The arrows correspond to the spins quantized along the z axis. The wave function of the carriers is given by

$$\Psi=\Psi_s|S\rangle+\mathbf{\Psi}_p|\mathbf{P}\rangle, \tag{2}$$

where Ψ_s and $\mathbf{\Psi}_p$ are the spinors. In the vicinity of the center of the Brillouin zone, equations for the envelope functions Ψ_s and $\mathbf{\Psi}_p$ can be written in the spherical approximation

$$\begin{aligned}
&(E-E_c)\Psi_s-\gamma\mathbf{k}\cdot\mathbf{\Psi}_p+\tfrac{1}{2}\hbar\omega\sigma_z\Psi_s=0,\\
&-\gamma\mathbf{k}\Psi_s+(E+\delta-E_v)\mathbf{\Psi}_p-i\delta[\boldsymbol{\sigma},\mathbf{\Psi}_p]+\tfrac{1}{2}\hbar\omega\sigma_z\mathbf{\Psi}_p\\
&+\frac{\hbar^2}{2m}(\gamma_1-2\gamma_2)k^2\mathbf{\Psi}_p+\frac{\hbar^2}{2m}6\gamma_3\mathbf{k}(\mathbf{k}\cdot\mathbf{\Psi}_p)=0.
\end{aligned} \tag{3}$$

Here γ is Kane's matrix element,[14] γ_1 and $\gamma_2=\gamma_3$ are the generalized Luttinger parameters,[14] $\delta=\Delta_{so}/3$, Δ_{so} is the spin-orbit splitting, E_c and E_v are the conduction and valence band-edge energies, m is the free electron mass, $\boldsymbol{\sigma}=(\sigma_x,\sigma_y,\sigma_z)$ are the Pauli matrices, $\mathbf{k}=-i\nabla-(e/(\hbar c))\mathbf{A}$, e is the electron charge, $\mathbf{A}$ is the vector potential of the magnetic field of strength H directed along the z axis, and $\omega=|e|H/(mc)$ is the cyclotron frequency. In the first equation of the system (3) we neglect the free electron mass term. If the heavy hole mass describing the interaction with the higher bands is introduced phenomenologically instead of the Luttinger parameters, the system (3) is to be transformed into the equations derived by Suris.[15] It can be shown that Eqs. (3) are identical to those commonly used.[14,16–18] Let $E_v=\delta$ and $E_c=E_g+\delta$, where E_g is the semiconductor band gap. By choosing the vector potential $\mathbf{A}=(-Hy,0,0)$ corresponding to magnetic field of strength $\mathbf{H}=(0,0,H)$, one can find that $\mathbf{k}=-i\nabla-(y/\lambda^2,0,0)$, where λ is the quantum magnetic length defined by $\lambda^2=\hbar/(m\omega)$.

We first present the solution of system (3) for a homogeneous semiconductor in a magnetic field. A Fourier transform can be performed in the plane (x,z) with the wave function presented in the form $\Psi=\exp(ik_x x+ikz)\Phi$. Here k_x and k are the wave vectors along the x and z axes, respectively. Let us introduce the operator $p=l+j_z$, where $l=c^\dagger c$,

$$j_z=-i\frac{\partial}{\partial\varphi}+\frac{1}{2}\sigma_z \quad \text{and} \quad \varphi=\arctan\frac{y}{x}. \tag{4}$$

Here c and $c^\dagger$ are the harmonic oscillator raising and lowering operators,[19] and j_z, which is the z-axis projection of the total angular momentum, is equal to the sum of the z-axis projections of the orbital angular momentum and the spin angular momentum of the electron. It can be shown that the operator p commutes with the Hamiltonian of the system. Therefore, the eigenvalues of the operator p are the same for each component of the wave function. Thus the wave function can be written in the basis of eigenfunctions of the total angular momentum:

$$\Phi=\sum_{i=1}^{8}F_i f_{l-j_{zi}}(\zeta)|j_i j_{zi}\rangle. \tag{5}$$

Here $f_l(\zeta)=\exp(-\zeta^2/2)H_l(\zeta)$ is the harmonic oscillator function, H_l is the Hermite polynomial, and $\zeta=y/\lambda-\lambda\ k_x$ is the normalized coordinate. In this way the wave vector k_x just shifts the origin of harmonic oscillator function. The wave function (5) is to be transformed to the basis (1) in order to substitute into the system (3) and obtain energy spectra and wave function coefficients of carriers. The basis transformation can be found in Ref. 19. The energy spectra

and wave functions are given in the Appendix. The quantum well can be presented in the following form:

$$|z|<a/2: \quad E_c=E_g+\delta, \quad E_v=\delta, \quad \Delta_{\mathrm{SO}}=3\delta,$$
$$|z|>a/2: \quad E_c=E_g+\delta+V_c, \quad E_v=\delta-V_v, \quad \Delta_{\mathrm{SO}}=3\tilde{\delta}. \tag{6}$$

The magnetic field is applied normally to the quantum well plane. The wave function is given by

$$\Psi=e^{ik_x x}e^{ikz}\Phi\pm e^{ik_x x}e^{-ikz}S\Phi \tag{7}$$

in the quantum well region. The factors $\exp(\pm ikz)$ in (7) have to be replaced by $\exp(-\kappa|z|)$ in the barrier regions. The plus and minus signs in (7) correspond to different wave function symmetries in the quantum well. The matrix S can be written as a direct product $S=P\otimes R$, where the matrix P acts on the coordinate components, and the matrix R on the spinor components of the wave function. By substituting $-k$ for k and $S\Phi$ for Φ, we can obtain $P=\mathrm{diag}(1,1,1,-1)$ from the first equation of the system (3) and then $R=\sigma_z=\mathrm{diag}(1,-1)$ from the second equation. Thus, the matrix S in the basis (1) is given by

$$S=\mathrm{diag}(1,-1,1,-1,1,-1,-1,1). \tag{8}$$

Some approximate methods to derive boundary conditions for quantum well heterostructures have been developed recently. Usually Kane's parameter γ varies only slightly in $A_{\mathrm{III}}B_{\mathrm{V}}$ semiconductor heterostructures. Hence γ is often supposed to be continuous[14]. For the sake of simplicity, we also consider that generalized Luttinger parameters γ_1 and γ_2 and dielectric constant κ_0 (see below) are continuous across the heteroboundaries. As shown in Ref. 12, the difference between Kane's parameters in the quantum well and barrier region almost does not change the Auger recombination coefficient. It is also shown in Ref. 12 that taking into account the difference between the dielectric constants in these regions influences only slightly the Auger recombination coefficient. Following the method elaborated by Burt[16] and assuming the continuity of Kane's parameter, the equations that can be integrated across the heterobarrier are derived from the system (3). Using these equations and the probability flux density conservation law, the boundary conditions for the wave function envelopes can be derived. The boundary conditions require the continuity at the heteroboundaries for the following quantities:

$$\gamma\Psi_{pz},$$
$$(\gamma_1-2\gamma_2)\frac{\partial}{\partial z}\Psi_{px},$$
$$(\gamma_1-2\gamma_2)\frac{\partial}{\partial z}\Psi_{py}, \tag{9}$$
$$\gamma\Psi_s+\frac{\hbar^2}{2m}6\gamma_2\frac{E_c-E}{\gamma}\Psi_s+i\frac{\hbar^2}{2m}(\gamma_1-2\gamma_2)\frac{\partial}{\partial z}\Psi_{pz},$$
$$(\gamma_1-2\gamma_2)\Psi_{px},$$
$$(\gamma_1-2\gamma_2)\Psi_{py}.$$

The wave function of the electron can be written as a linear combination of two wave functions corresponding to two spin orientations of the electron. Neglecting Luttinger parameters, we can find from the boundary conditions (9) that the components Ψ_s and Ψ_{pz} of the wave function of electron must be continuous at the heteroboundaries. The dispersion equation obtained from these boundary conditions for electrons is given in the Appendix.

The wave function of the hole is a superposition of three subbands of the valence band: heavy, light, and SO holes. However, the last subband decays exponentially away from the heteroboundary. As a consequence, this branch mainly affects the derivative of wave function near the heteroboundary, and its influence on the wave function itself is negligible. Thus, we can seek for the wave function as a superposition of the heavy hole and light hole subbands. Near the upper edge of the valence band, $m_l \ll m_h$ [m_l and m_h are defined by Eq. (A12) in the Appendix]. This means that the second and third of the boundary conditions (9) are inapplicable. In this approximation, light and heavy holes do not mix with each other and have different spectra.[12] The heavy hole spectrum coincides with the quantum-mechanical spectrum of a particle in a rectangular quantum well. The dispersion equation for heavy holes is given in the Appendix.

III. AUGER RECOMBINATION COEFFICIENTS

The probability of Auger recombination in terms of first-order perturbation theory is given by the following expression:

$$W_{fi}=\frac{2\pi}{\hbar}|M_{fi}|^2\delta(E_f-E_i), \tag{10}$$

where

$$M_{fi}=\left\langle \Psi_f(\mathbf{r_1},\mathbf{r_2})\left|\frac{e^2}{\kappa_0|\mathbf{r_1}-\mathbf{r_2}|}+\varphi(\mathbf{r_1},\mathbf{r_2})\right|\Psi_i(\mathbf{r_1},\mathbf{r_2})\right\rangle \tag{11}$$

is the matrix element of the Coulomb interaction, $\mathbf{r}_1$ and $\mathbf{r}_2$ are the coordinates of carriers, and $\varphi(\mathbf{r}_1,\mathbf{r}_2)$ is the additional potential arising from the difference between the quantum well dielectric constant κ_0 and the barrier region dielectric constant $\tilde{\kappa}_0$. An explicit expression for $\varphi(\mathbf{r_1},\mathbf{r_2})$ is derived in Ref. 12.

Taking into account the antisymmetrized forms of the wave functions, the matrix element (11) becomes the following:

$$M_{fi}=M^{\mathrm{I}}-M^{\mathrm{II}}, \tag{12}$$
$$M^{\mathrm{I}}=\left\langle \Psi_3(\mathbf{r_1})\Psi_4(\mathbf{r_2})\left|\frac{e^2}{\kappa_0|\mathbf{r_1}-\mathbf{r_2}|}+\varphi(\mathbf{r_1},\mathbf{r_2})\right|\Psi_1(\mathbf{r_1})\Psi_2(\mathbf{r_2})\right\rangle, \tag{13}$$

and expression for M^{II} can be obtained from (13) by interchange of indices 1 and 2 in the arguments of wave functions Ψ_1 and Ψ_2.

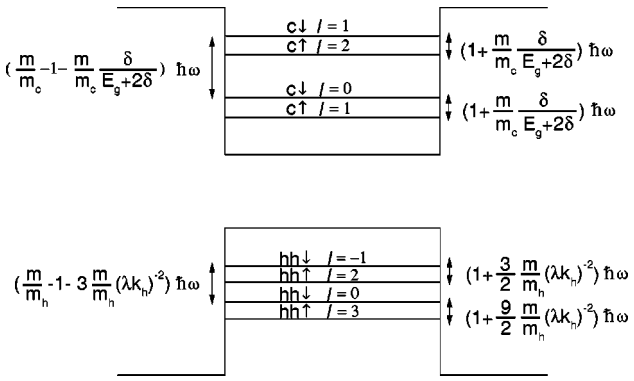

FIG. 1. Ground states of charge carriers in a semiconductor quantum well with perpendicularly applied magnetic field.

We now consider the CHCC process of Auger recombination. Only a small number of ground states (the first size quantization level and few first Landau levels) participate in the Auger process at sufficiently low temperatures. These ground states are shown in Fig. 1. There are two dominant types of transitions which occur between the following states:

$$(c_\uparrow,+,l=p+1,k_c,k_{x1})+(c_\downarrow,-,l=s,k_r,k_{x2}) \rightarrow (c_\uparrow,+,l=n+1,k_f,k_{x3})+(hh_\downarrow,-,l=t-1,k_h,k_{x4}), \tag{14}$$

$$(c_\downarrow,-,l=p,k_c,k_{x1})+(c_\uparrow,+,l=s+1,k_r,k_{x2}) \rightarrow (c_\downarrow,-,l=n,k_f,k_{x3})+(hh_\uparrow,+,l=t+2,k_h,k_{x4}). \tag{15}$$

Here the symbols $c_\uparrow$, $c_\downarrow$, $hh_\uparrow$, and $hh_\downarrow$ identify the branches of the electron and heavy hole spectra; the signs plus and minus denote the symmetries of wave functions (7) in the quantum well; k_c, k_r, k_f, and k_h are the wave vectors of size quantization ground states; $k_{x1}, \ldots, k_{x4}$ are the x-axis wave vectors; l is the Landau level index; and $p,s,n,t=0,1,2,\ldots$ The number n may be equal to, or greater than, 0, and equal to, or less than, $n_{\max}\cong 2E_g/(\hbar\omega_c)\gg 1$, according to the energy conservation law (ω_c is defined in the Appendix). We consider two main cases: (1) $n=0,1,2,\ldots$ (transition to continuous spectrum states) and (2) $n\cong n_{\max}$ (transition to discrete spectrum states). Both processes are shown in Fig. 2. According to the dispersion equations (see the Appendix), $k_c\cong k_r<k_f\approx k_h$ for the first case and $k_c\cong k_r \simeq k_f<k_h$ for the second.

A. Transition into the continuous spectrum

The Auger transition to continuous spectrum states corresponds to the following conditions for the index n and wave vectors of carriers

$$n=0,1,2,\ldots \quad \text{and} \quad k_c\cong k_r<k_f\approx k_h. \tag{16}$$

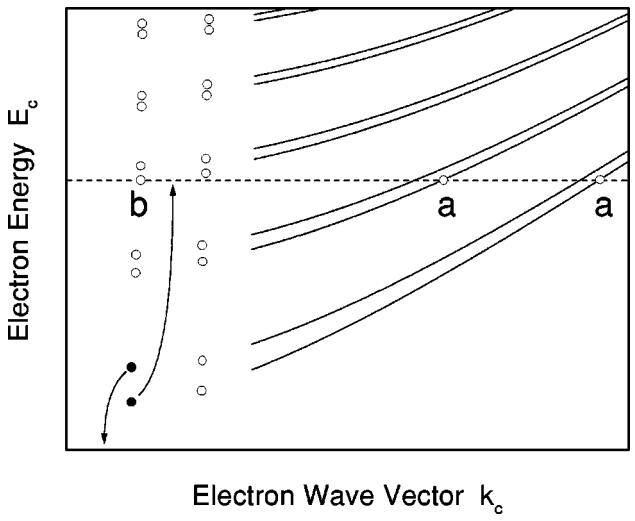

FIG. 2. CHCC Auger process in a semiconductor quantum well with perpendicularly applied magnetic field. (a) A transition to a continuous spectrum state, (b) a transition to a discrete spectrum state. Here E_c is the energy of the electron, and k_c the wave vector of the electron.

By substituting the wave functions given by (A1), (A7), and (A18) for the process (14) into matrix element (13) and using approximation $V_{c,v}\ll E_g$, we obtain

$$M^{\mathrm{I}}\cong \frac{2^{1/2}e^2\gamma}{\pi^3\kappa_0 E_g X^2 Z^{1/2}\lambda^3 a^{3/2}}(2^{n+p+s+t}n!p!(s+1)!t!)^{-1/2}I, \tag{17}$$

where

$$\begin{aligned} I=&\int\int\int_{\mathbf{R}^3} q^{-2}e^{i\mathbf{q}(\mathbf{r}_1-\mathbf{r}_2)}d^3q \\ &\times\int\int_{\mathbf{R}^2} e^{i(k_{x1}-k_{x3})x_1}e^{i(k_{x2}-k_{x4})x_2}dx_1dx_2 \\ &\times\int\int_{\mathbf{R}^2} f_p(y_1/\lambda-\lambda k_{x1})f_n(y_1/\lambda-\lambda k_{x3}) \\ &\times f_{s+1}(y_2/\lambda-\lambda k_{x2})\times f_t(y_2/\lambda-\lambda k_{x4})dy_1\,dy_2 \\ &\times\int\int_{\mathbf{R}^2}\phi(k_cz_1)\phi(k_fz_1)\phi(k_rz_2)\phi(k_hz_2)\,dz_1\,dz_2, \end{aligned} \tag{18}$$

X and Z are normalization constants, and

$$\begin{aligned} |z|<a/2:&\quad \phi(k_{c,f,r,h}z)=\cos(k_{c,f,r,h}z), \\ |z|>a/2:&\quad \phi(k_{c,r}z)=e^{-\kappa_{c,r}|z|}, \\ &\phi(k_fz)=\cos(k_fz),\quad \phi(k_fz)=0. \end{aligned} \tag{19}$$

Here and in the following we drop the prefactor:

$$\left(1-\frac{\gamma^2((k_f-k_c)^2+k_r^2)}{2E_g^2}\right)\frac{E_g}{E_g-\delta}\left(1+2t\frac{k_r}{k_h}\right), \tag{20}$$

which is about 1 in formulas for the matrix element M^{I}.

At sufficiently low temperatures ($T \ll \hbar\omega_c$), when the magnetic field effects become important, we can take into account only the ground Landau levels of the initial states, $p=0$ and $s=0$. In this approximation we still obtain a result of correct order, reflecting important features of the matrix element as a function of temperature, magnetic field strength, and heterostructure parameters. However, for these levels the limit $H \to 0$ is equivalent to the limit $k_{x,y} \to 0$ in the absence of magnetic field.[20] Note that the index t takes all values between 0 and ∞ due to the condition $\hbar\omega_h \ll \hbar\omega_c$, and so does n (ω_h is defined in the Appendix). We also suppose that the magnetic field is not too high so that the Landau level coupling is much less than the size quantization energy $\hbar\omega \ll \hbar^2 k^2/2m$. This condition can be written in the form $a^2 \ll \lambda^2$. Then $q_z^2 \gg q_x^2 + q_y^2$, and the factor q^{-2} in (18) can be expanded into the series $q^{-2} \cong q_z^{-2} - (q_x^2 + q_y^2) q_z^{-4}$. Using these approximations, the integral (18) can be easily calculated as

$$I \cong (-1)^n 2^{2-[(n+t)/2]} \pi^{9/2} \lambda e^{-k_{13}^2 - k_{14}^2} H(k_{34}, k_{13}) J \times \delta(k_{x1} + k_{x2} - k_{x3} - k_{x4}) \tag{21}$$

with the help of integral tables.[21] Here $k_{ij} = \lambda(k_{xi} - k_{xj})/\sqrt{2}$ $(i,j = 1, \ldots, 4)$,

$$J = q_l^{-1} \int \int_{\mathbf{R}^2} \phi(k_c z_1)\, \phi(k_f z_1)\, \phi(k_r z_2)\, \phi(k_h z_2) \times e^{-q_l |z_1 - z_2|}\, dz_1\, dz_2, \tag{22}$$

$$H(k_{34}, k_{13}) = H_{n+t+1}(k_{34}) + 4k_{13} H_{n+t}(k_{34}) + 4t H_{n+t-1}(k_{34}), \tag{23}$$

$$q_l^2 = -[H_{n+t+3}(k_{34}) + 8k_{13} H_{n+t+2}(k_{34}) + 4(4k_{13}^2 + t) \times H_{n+t+1}(k_{34}) - 4tk_{13} H_{n+t}(k_{34})]/[2\lambda^2 H(k_{34}, k_{13})], \tag{24}$$

and $H_n(k)$ is a Hermite polynomial.

An approximate expression for the integral (22) can be obtained by integration by parts over the z_1 coordinate.[12] We again use the approximation $V_{c,v} \ll E_g$. Then (22) becomes

$$J \cong J_1 + J_2, \tag{25}$$

where

$$J_1 = F(a/2) \int_{-a/2}^{a/2} \phi(k_h z)\, \phi(k_r z)\, e^{q_l z}\, dz - F(-a/2) \int_{-a/2}^{a/2} \phi(k_h z)\, \phi(k_r z)\, e^{-q_l z}\, dz, \tag{26}$$

$$F(\pm a/2) = \mp \frac{2}{k_f^2 + q_l^2} e^{-q_l a/2} \phi(\pm k_f a/2)\, \phi(\pm k_c a/2) \times \left(\frac{3V_c + V_v}{4E_g} - \frac{\kappa_0 - \tilde{\kappa}_0}{\kappa_0 + \tilde{\kappa}_0} \right), \tag{27}$$

$$J_2 = \frac{2}{k_f^2 + q_l^2} \int_{-a/2}^{a/2} \phi(k_h z)\, \phi(k_r z)\, \phi(k_f z)\, \phi(k_c z)\, dz. \tag{28}$$

The term $(\kappa_0 - \tilde{\kappa}_0)/(\kappa_0 + \tilde{\kappa}_0)$ in Eq. (27) arises from taking into account the additional potential $\varphi(\mathbf{r_1}, \mathbf{r_2})$ in Eq. (13) (see Ref. 12).

Expression (25) shows that the matrix element splits into two terms. The first term J_1 is related to the presence of heteroboundaries, and the second term J_2 corresponds to the short-range Coulomb scattering. The latter is conditioned by the fact that large energy is transferred in Auger transition and this is possible only if the scattering particles find themselves very close to each other. We suppose that $a^2 \ll \lambda^2$, and therefore, $q_l z \ll 1$ in J_1 which corresponds to scattering at both heteroboundaries simultaneously. Calculation of the integrals J_1 and J_2 gives

$$J_1 \cong \frac{8k_h}{(k_f^2 + q_l^2)(k_h^2 + q_l^2)} \frac{k_c k_r}{\sqrt{(k_c^2 + \kappa_c^2)(k_r^2 + \kappa_r^2)}} \times \left(\frac{3V_c + V_v}{4E_g} - \frac{\kappa_0 - \tilde{\kappa}_0}{\kappa_0 + \tilde{\kappa}_0} \right) \cos(k_f a/2),$$

$$J_2 \cong -\frac{k_h}{(k_f^2 + q_l^2)((k_f - k_c - k_r)^2 - k_h^2)} \cos((k_f - k_c - k_r) a/2), \tag{29}$$

where we use conditions (16) to ignore six less significant terms of the eight ones in J_2 and the boundary conditions (A22) to express $\phi(\pm k_j a/2)$ in J_1.

Both terms J_1 and J_2 are thresholdless matrix elements. Indeed, there are no restrictions imposed on the initial momenta of carriers. However, the mechanisms responsible for the momentum nonconservation in J_1 and J_2 are different. The mechanism in J_1 is related to carrier scattering at the heteroboundary. The same reason gives rise to a thresholdless Auger process in scattering on a single heterobarrier point.[10] The mechanism in J_2 is determined by the restriction of the volume of integration with respect to the z coordinate to the quantum well region. This restriction results in the appearance of a function of the type $k^{-1} \sin(ka/2)$ instead of the delta function $\delta(k)$.

The probabilities of Auger transition (10) have to be summed over all initial and final states of charge carriers to obtain the Auger recombination rate. This sum can be written as the integral

$$G = \frac{1}{XY} \frac{2\pi}{\hbar} \int |M_{fi}|^2 \delta(E_f - E_i)\, \mathrm{F} d\Gamma \tag{30}$$

with the density of states

$$\mathrm{F} d\Gamma = n_c XY \frac{dk_{x1}}{K_X} n_r XY \frac{dk_{x2}}{K_X} \frac{K_X K_Z XZ}{(2\pi)^2} \frac{dk_{x3} dk_f}{K_X K_Z} n_h XY \frac{dk_{x4}}{K_X}. \tag{31}$$

Here K_X, K_Z and $Y = \lambda^2 K_X$ are normalization constants; n_c, n_r, and n_h are the densities of electrons and holes; M_{fi} is the

matrix element defined by (12) and (13); $E_i=E_1+E_2$ and $E_f=E_3+E_4$ are the initial and final energies of the system, respectively; and indices $1,\ldots,4$, c, r, f, h are the same as those used in (14) and (15). The rate (30) is to be summed over the indices n and t. The matrix element M_{fi} in (30) can be written as the sum

$$M_{fi}=M_1^{\mathrm{I}}-M_1^{\mathrm{II}}+M_2^{\mathrm{I}}-M_2^{\mathrm{II}}+M_3^{\mathrm{I}}-M_3^{\mathrm{II}}, \tag{32}$$

where the terms M^{II} can be calculated similarly to M^{I} by interchanging the indices 1 and 2 in the arguments of wave functions Ψ_1 and Ψ_2 in (13). However, the terms M^{II} are negligible with respect to the corresponding terms M^{I} for processes (14) and (15) due to the small coupling between states $c_\uparrow$ and $c_\downarrow$. The terms M_1 and M_2 correspond to the terms J_1 and J_2 [see (21) and (25)], and the term M_3 is derived below for the Auger transition to discrete spectrum states.

The contributions to the Auger rate (30) from the matrix elements M_1 and M_2, on the one hand, and M_3, on the other, can be separated. The reason is that these matrix elements describe transitions of a particle to a continuous or discrete spectrum state, respectively. Separating the contributions from M_1 and M_2 is more difficult. Even though there is a physical difference between these matrix elements, a term of interference between them appears in the total Auger rate (30). However, neglecting the interference between M_1 and M_2, we still obtain the result of correct order, reflecting all important features of the Auger recombination rate as a function of magnetic field strength, temperature, and parameters of a quantum well structure.

According to the aforesaid, the rate of Auger recombination can be written as the sum

$$G=G_1+G_2+G_3, \tag{33}$$

where the terms G_j correspond to the matrix elements M_j $(j=1,\ldots,3)$. The rate G_3 will be derived below. The rates G_1 and G_2 can be obtained from (30) and (31) by substituting the matrix elements M_1 and M_2 from (12), (17), (21), (23), (25), and (29). The substitution gives

$$G_i\cong n_c n_r n_h \frac{e^4\gamma^2}{\kappa_0^2\hbar E_g^2 a^3}\frac{4\pi}{2^{2(n+t)}n!t!}Q_i^2 I_{xi}I_z, \tag{34}$$

$$I_{xi}=K_X^{-1}\int\int\int\int_{\mathbf{R}^4}L_i^2H^2(k_{34},k_{13})\,\delta(k_{x1}+k_{x2}-k_{x3}-k_{x4}) \times e^{-2k_{13}^2-2k_{34}^2}dk_{x1}\,dk_{x2}\,dk_{x3}\,dk_{x4}, \tag{35}$$

$$I_z=\int_{\mathbf{R}}\delta(E_3+E_4-E_1-E_2)\,dk_f. \tag{36}$$

Here $i=1,2$ and the matrix elements J_i from (29) are factorized as the following product:

$$J_i=L_iQ_i, \quad \text{where } Q_i\equiv J_i\big|_{q_l=0}. \tag{37}$$

In the case $a^2\ll\lambda^2$, the factors L_1 and L_2 can be written as a Taylor series in the small parameter q_l^2/k_z^2. Ignoring high-order terms, we can derive from (29) and (37)

$$L_i=1-K_i^{-2}q_l^2, \quad \text{where } K_1^{-2}=k_h^{-2}+k_f^{-2} \text{ and } K_2^{-2}=k_f^{-2}. \tag{38}$$

Calculation of the integrals (35) and (36) gives

$$I_{xi}=\pi\lambda^{-2}2^{n+t+1}[(n+t+1)!-4nt(n+t-1)! -\lambda^{-2}\mathrm{K}_i^{-2}(2(n+t+2)!-3t(n+t+1)!-2t^2(n+t)!)] \tag{39}$$

and

$$I_z\cong 2^{-3/2}3\,\gamma^{-1} \tag{40}$$

with the help of integral tables.[21]

The Boltzmann distribution often takes place for holes. Taking into account the heavy hole spectrum (A17), we can write for the densities n_c, n_r, and n_h

$$n_c\cong n_r\cong\frac{n}{2} \quad \text{and} \quad n_h\cong\frac{p}{2}e^{-(\hbar\omega_h/T)t}(1-e^{-\hbar\omega_h/T}). \tag{41}$$

In what follows we study the Auger coefficients C_i instead of the Auger rates G_i, related by $G_i=n^2pC_i$. The expressions for the Auger coefficients C_1 and C_2 obtained by substituting (29) and (37)–(41) into (34) and summing over the indices n and t are given by

$$C_i=2^{1/2}3\pi^2\frac{e^4\gamma}{\kappa_0^2\hbar E_g^2a^3\lambda^2}Q_i^2\left(1-\frac{8N}{\lambda^2\mathrm{K}_i^2}\right), \tag{42}$$

where

$$N=\frac{9}{8}\frac{1}{1-e^{-\hbar\omega_h/T}}-\frac{1}{8}. \tag{43}$$

The same expression can be obtained for process (15). The only difference is the correction factor

$$\left(1-\frac{\gamma^2((k_f-k_c)^2+k_r^2)}{2E_g^2}\right)\frac{E_g^2}{(E_g-\delta)(E_g+2\delta)}2\frac{k_r}{k_h} \tag{44}$$

instead of (20). Summation of the Auger coefficients (42) for both processes (14) and (15) gives the final expressions

$$C_1=2^{13/2}3\pi^2\frac{e^4\gamma}{\kappa_0^2\hbar E_g^2a^3\lambda^2}\frac{k_c^4}{k_f^4k_h^2(k_c^2+\kappa_c^2)^2} \times\left(\frac{3V_c+V_v}{4E_g}-\frac{\kappa_0-\tilde{\kappa}_0}{\kappa_0+\tilde{\kappa}_0}\right)^2\left(1-8N\frac{k_f^2+k_h^2}{\lambda^2k_f^2k_h^2}\right) \tag{45}$$

and

$$C_2 = 2^{1/2} 3\pi^2 \frac{e^4\gamma}{\kappa_0^2 \hbar E_g^2 a^3 \lambda^2} \frac{k_h^2}{k_f^4((k_f-2k_c)^2-k_h^2)^2} \times (1+\cos((k_f-2k_c)a))\left(1-\frac{8N}{\lambda^2 k_f^2}\right). \quad (46)$$

B. Transition into the discrete spectrum

The Auger transition to discrete spectrum states corresponds to the following conditions for the index n and the wave vectors of charge carriers:

$$n \cong (E_g\lambda/\gamma)^2 \gg 1 \quad \text{and} \quad k_c \cong k_r \simeq k_f < k_h. \quad (47)$$

The matrix element of the process (14) is given by the same expressions (17) and (18) with the quantum well width a substituted for Z. The integrals over x_1, x_2, q_x, y_1, and y_2 in (18) can be calculated by the same method as that used for transition into the continuous spectrum. The only difference is the integral over q_y. It can be shown that $q_y^2 \propto \ln(n) E_g^2/\gamma^2$ in the case $a^2 \ll \lambda^2$. This means that $q_z^2 \ll q_y^2$ and therefore the factor q^{-2} in (18) can be expanded into the series $q^{-2} \cong q_y^{-2} - (q_z^2+q_x^2) q_y^{-4}$. Calculation of the integrals over q_z, z_1, z_2, and q_y gives a result similar to (21), (25), and (29). However, due to the condition $q_z^2 \ll q_y^2$, the term J_1 can be neglected compared with the term J_2. The final expression for the integral (18) is of the form

$$I \cong (-1)^{n+1} 2^{4-[(n+t)/2]} \pi^{9/2} a \lambda^3 e^{-k_{13}^2 - k_{14}^2} H(k_{34}) A \times \delta(k_{x1}+k_{x2}-k_{x3}-k_{x4}). \quad (48)$$

Here $k_{ij} = \lambda(k_{xi}-k_{xj})/\sqrt{2}$ $(i,j=1,\ldots,4)$,

$$A = \frac{i}{16} \sum_{s_{1,\ldots,4}=\pm 1} \frac{\sin((s_1 k_e + s_2 k_r + s_3 k_f + s_4 k_h)a/2)}{(s_1 k_c + s_2 k_r + s_3 k_f + s_4 k_h)a/2}, \quad (49)$$

$$H(k_{34}) = H_{n+t-1}(k_{34}) + 2(\lambda^2 k_c^2 + 2t) H_{n+t-3}(k_{34}). \quad (50)$$

The rate of the Auger recombination is given by (30) with the density of states

$$\mathrm{F}d\Gamma = n_c XY \frac{dk_{x1}}{K_X} n_r XY \frac{dk_{x2}}{K_X} \frac{K_X X}{2\pi} \frac{dk_{x3}}{K_X} n_h XY \frac{dk_{x4}}{K_X}, \quad (51)$$

which is different from (31). Substituting (12), (17), (48), (50), and (51) into (30) and integrating over $k_{x1}, \ldots, k_{x4}$, we obtain the Auger recombination coefficient

$$C_3 = (2\pi)^3 \frac{e^4\gamma^2\lambda^2}{\kappa_0^2 \hbar E_g^2 a^2} (1-e^{-(\hbar\omega_h/T)}) e^{-(\hbar\omega_h/T)t} A^2 \times \frac{(n+t-1)! + (\lambda^2 k_c^2 + 2t)^2 (n+t-3)!}{2^n 2^t n! t!} \delta(E_f - E_i). \quad (52)$$

Here the delta function appears because of the entirely discrete spectrum of the system. The delta function can be written in the following form:

$$\delta(E_f - E_i) = \frac{\hbar\Gamma}{\pi(\hbar^2\Gamma^2 + (E_f-E_i)^2)}, \quad (53)$$

where Γ is the normal width of the transition. The Auger recombination coefficient (52) is to be summed over the indices n and t, taking into account that the final energy E_f depends on the index n, and the initial energy E_i on the index t. The result of this summing is quite different in two limiting cases $\Gamma \ll \omega$ and $\Gamma \gg \omega$. We calculate this sum numerically in the next section. Let us present here only the expression for the difference of the final and initial energies of the system

$$E_f - E_i = \varepsilon_{c\uparrow}(k_f, l=n+1) + \varepsilon_{hh\downarrow}(k_h, l=t-1) - \varepsilon_{c\uparrow}(k_c, l=1) - \varepsilon_{c\downarrow}(k_r, l=0) - E_g. \quad (54)$$

The terms $\varepsilon_{c\uparrow}$, $\varepsilon_{c\downarrow}$, $\varepsilon_{hh\uparrow}$, and $\varepsilon_{hh\downarrow}$ are given by (A6) and (A17).

The same coefficient (52) can be obtained for process (15). The energy difference for this process is given by

$$E_f - E_i = \varepsilon_{c\downarrow}(k_f, l=n) + \varepsilon_{hh\uparrow}(k_h, l=t+2) - \varepsilon_{c\downarrow}(k_c, l=0) - \varepsilon_{c\uparrow}(k_r, l=1) - E_g. \quad (55)$$

IV. RESULTS

Let us consider in detail the Auger recombination coefficients C_1, C_2, and C_3 given by (45), (46), and (52), respectively. The dependencies of these three coefficients on the magnetic field strength, quantum well width, and temperature are shown in Figs. 3, 4, and 5, respectively. Here the coefficients C_1 and C_2 (Figs. 3 and 4) are calculated for GaAs–GaAlAs heterostructures ($E_g = 1.52$ eV, $m_c = 0.07m$, $m_h = 0.68m$, $\delta = 0.1$ eV, $V_c = 0.1$ eV, $V_v = 0.1$ eV, $\kappa_0 = 10$), and the coefficient C_3 (Fig. 5) for InSb–InGaSb heterostructures ($E_g = 0.23$ eV, $m_c = 0.016m$, $m_h = 0.40m$, $\delta = 0.3$ eV, $V_c = 0.1$ eV, $V_v = 0.1$ eV, $\kappa_0 = 10$, $\Gamma = 10^{12}\mathrm{s}^{-1}$). The same InSb–InGaSb heterostructure is used below in Fig. 6.

All three Auger recombination processes are thresholdless. Indeed, in the limit of zero temperature all coefficients

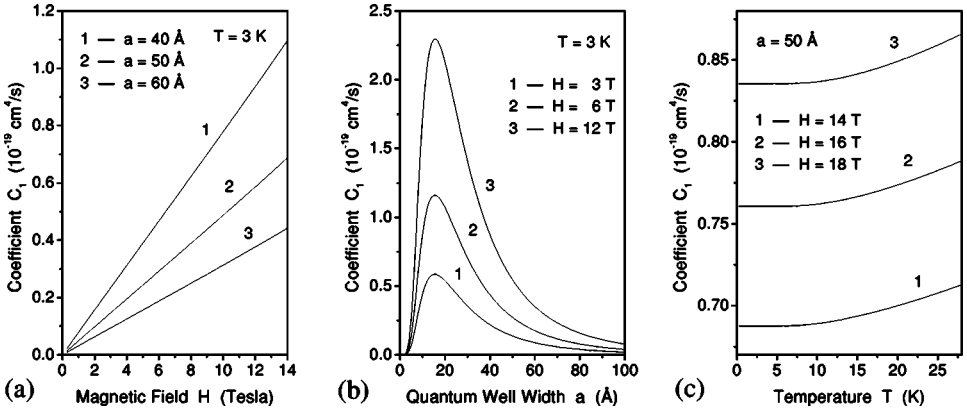

FIG. 3. Auger recombination coefficient C_1 for electron scattering on interband with transition into continuous spectrum as a function of (a) magnetic field, (b) quantum well width, and (c) temperature in GaAs–GaAlAs heterostructures. Here H is the magnetic field strength in Tesla, a is the quantum well width in Å, and T is temperature in K; the same for Figs. 4–6.

have nonzero values [see Figs. 3(c), 4(c), and 5(c)]. However, the reasons for the absence of a threshold are different for the transitions to continuous and discrete spectrum states. The threshold arises because a large momentum has to be transferred in Auger recombination by virtue of the energy and momentum conservation principles. For the transition into the continuous spectrum, the presence of a quantum well removes the conservation principle for the momentum component normal to heteroboundaries. For the transition into the discrete spectrum, the transferred momentum is small because the final electron in a sufficiently high Landau level has the momentum approximately equal to that of the initial electron.

The coefficients C_1 and C_2 increase, and the coefficient C_3 oscillates, with magnetic field strength [see Figs. 3(a), 4(a), and 5(a)]. These effects can be explained as follows. As it is known from the quantum mechanics, the magnetic field localizes wave functions. The localization makes the Coulomb matrix element larger, and the Auger recombination rate higher, compared with the case without magnetic field. The reason for the oscillations of the coefficient C_3 is the resonant nature of the Auger recombination process with a transition into the discrete spectrum. The process is thresholdless; however, a small factor 2^{-n} replaces the threshold factor $\exp(-E_{\rm th}/T)$ in the coefficient C_3. One can obtain from (47) that $n \cong 2E_g/(\hbar\omega_c)$, where $\omega_c = \omega m/m_c$ and m_c is the electron mass in the case of zero constant of spin-orbit interaction given by $m/m_c = 2m\gamma^2/(\hbar^2 E_g)$. The number n is usually much greater than unity in real fields. Thus, there is a threshold with respect to field, instead of temperature, owing to the factor $\exp(-H_{th}/H$ in the Auger coefficient C_3. Therefore, the amplitude of oscillations increases with magnetic field [see Fig. 5(a)]. Note that the local maximums of the coefficient C_3 as a function of magnetic field are smoother on the higher field side and sharper on the lower field side. The right-hand slopes of the local maximums reproduce the thermal distribution of heavy holes (Boltzmann distribution), because the energy of a high-Landau-level electron is much more sensitive to the magnetic field strength than the energy of a low-Landau-level heavy hole.

The Auger coefficients vanish when the magnetic field strength approaches zero [see Figs. 3(a), 4(a), and 5(a)]. The reason is the factor 2^{-n} in the coefficient C_3. In order to explain the behavior of the coefficients C_1 and C_2, let us compare these coefficients with the corresponding expressions derived in the absence of magnetic field:[12]

$$\frac{C_1(H)}{C_1(0)} \simeq \frac{3}{2}\frac{k_c^2 k_h^2}{\kappa_c^2(k_c^2+\kappa_c^2)}\frac{\hbar\omega_h}{T}, \quad \frac{C_2(H)}{C_2(0)} \simeq \frac{3}{4}\frac{k_h^2}{k_c^2}\frac{\hbar\omega_h}{T}. \tag{56}$$

One can see that the reciprocal quantum magnetic length λ^{-1} is to be replaced by the thermal momentum $q_T = \sqrt{2mT}/\hbar$ in order to obtain the correct limiting expressions. Indeed, the wave vectors of the electrons and holes are on the order of thermal momentum q_T owing to the interactions between charge carriers. On the other hand, transitions involving higher Landau levels of electrons have to be considered in the limit $H \to 0$.[20] Thus, the indices p and s of the

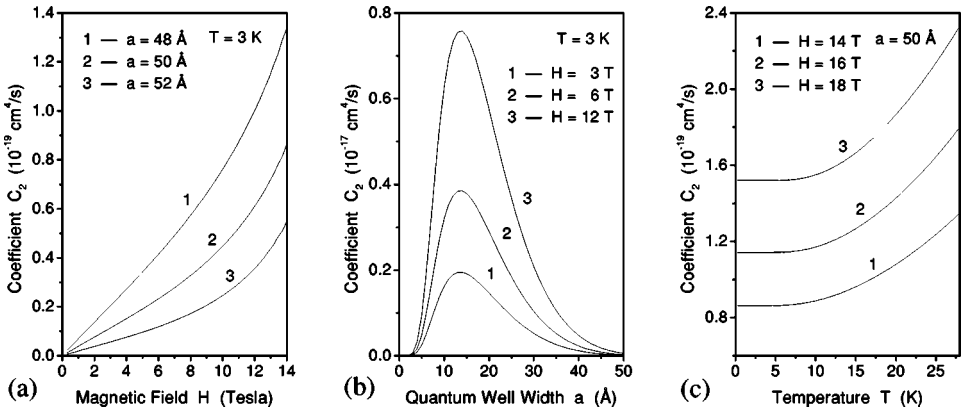

FIG. 4. Auger recombination coefficient C_2 for short-range Coulomb interaction in quantum well with transition into continuous spectrum as a function of (a) magnetic field, (b) quantum well width, and (c) temperature in GaAs–GaAlAs heterostructures.

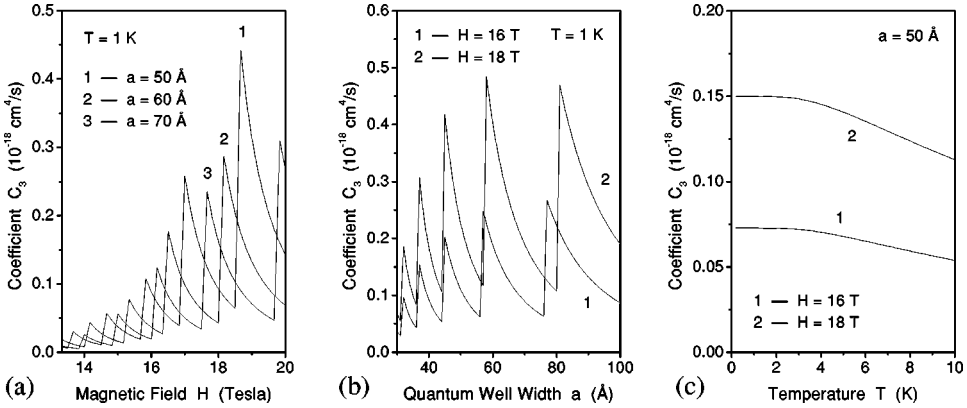

FIG. 5. Auger recombination coefficient C_3 for resonance transition into discrete spectrum as a function of (a) magnetic field, (b) quantum well width, and (c) temperature in InSb–InGaSb heterostructures.

initial electron states are on the order of $T/(\hbar\omega_c)$ instead of zero. This additionally decreases the Auger recombination coefficients.

Comparing Figs. 3(b) and 4(b), one can see that the coefficient C_2 decreases much faster than the coefficient C_1 with increasing quantum well width. Indeed, the following factor, a part of C_2, transforms into the delta function expressing the momentum conservation principle:

$$\frac{k_h^2(1+\cos((k_f-2k_c)a))}{a((k_f-2k_c)^2-k_h^2)^2}\rightarrow\frac{\pi}{4}\delta(k_f-2k_c-k_h) \quad (57)$$

when the quantum well width tends to infinity. The delta function then has to be averaged over the heavy hole distribution. As a result, the coefficient C_2 multiplied by a^2 transforms in the limit $H\rightarrow 0$ into a 3D expression derived for the bulk semiconductor in the absence of magnetic field.[2] On the other hand, a^2C_1 decreases as inverse quantum well width in the limit $a\rightarrow\infty$ due to the heteroboundaries moving away to infinity.

The coefficient C_3 is negligible in comparison with C_1 and C_2 for wide gap semiconductors in not too high magnetic fields owing to the factor 2^{-n}. Therefore, we have calculated the total Auger recombination coefficient $C=C_1+C_2+C_3$ shown in Fig. 6 for a heterostructure with narrow-gap semiconductor InSb. One can see that the process I dominates at higher fields and wider quantum wells, the process II dominates at lower fields and narrower quantum wells, and the process III becomes significant only at higher fields. The total Auger recombination coefficient C shows a rather complex dependence on magnetic field strength and quantum well width.

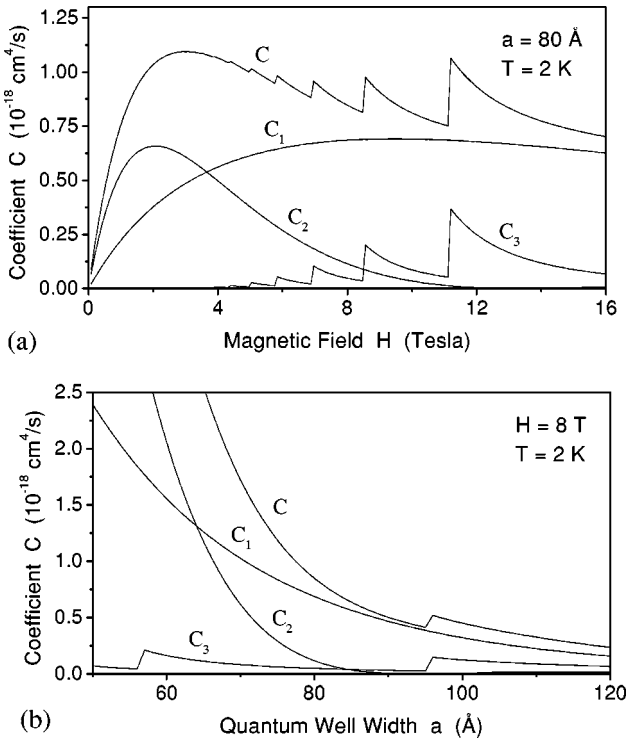

FIG. 6. Total Auger recombination coefficient as a function of (a) magnetic field and (b) quantum well width in InSb–InGaSb heterostructures.

V. CONCLUSIONS

In conclusion we have shown that three fundamentally different Auger recombination channels exist in semiconductor quantum wells with perpendicularly applied magnetic field. The Auger recombination coefficients have been calculated analytically for each of these channels. The calculations have been performed for the CHCC Auger process. A similar analysis of the CHHS process will be the subject of future work. A four-band Kane's model and the first-order perturbation theory were used to obtain the wave functions of charge carriers and to derive the probability of Auger recombination. The dependencies of the calculated Auger recombination coefficients on the magnetic field strength, quantum well parameters, and temperature are investigated. It is shown that all channels are of the threshold type. The limiting cases of an infinite quantum well width and negligible magnetic field strength are analyzed. It is shown that a reasonable agreement exists between the limiting expressions of formulas derived in the paper and the results known from the literature. The Auger recombination coefficients for the transition into continuous spectrum show a linear dependence on magnetic field broken down at too high (Landau quantization energy exceeds the size quantization energy) and too small (magnetic length much exceeds the heavy hole thermal momentum) magnetic field strength. These limiting cases will be the subject of future investigations. The Auger recombination coefficient for the transition into the discrete spectrum shows an oscillating dependence on the magnetic field strength owing to the resonant nature of the process.

ACKNOWLEDGMENTS

The authors thank A. S. Polkovnikov for valuable discussions. This work was partially supported by the Russian Foundation for Basic Research (Grant Nos. 98-02-18211, 98-07-90336, 99-02-16796, and 00-15-96812).

APPENDIX: WAVE FUNCTIONS OF CARRIERS

The wave function (5) is written in the basis of eigenfunctions of the total angular momentum. This wave function

$$\Phi=\begin{pmatrix} Mf_{l-1}(\zeta)|S\uparrow> \\ Nf_l(\zeta)|S\downarrow> \\ (Af_{l-2}(\zeta)+Bf_l(\zeta))|X\uparrow> \\ (Sf_{l-1}(\zeta)+Tf_{l+1}(\zeta))|X\downarrow> \\ i(Af_{l-2}(\zeta)-Bf_l(\zeta))|Y\uparrow> \\ i(Sf_{l-1}(\zeta)-Tf_{l+1}(\zeta))|Y\downarrow> \\ Cf_{l-1}(\zeta)|Z\uparrow> \\ Df_l(\zeta)|Z\downarrow> \end{pmatrix} \tag{A1}$$

transformed to basis (1) and multiplied by $\Omega^{-1}\exp(ik_x x+ikz)$ is to be substituted into the system (3) in order to obtain the spectra and wave function coefficients of carriers (see basis transformation in Ref. 19). Here Ω is the normalization constant. It is easy to show that

$$\Omega^2=\sqrt{\pi}2^{l-1}(l-2)!XZ(A^2+(l-1)(M^2+C^2+2S^2)+2l(l-1)(N^2+D^2+2B^2)+8(l+1)l(l-1)T^2). \tag{A2}$$

The substitution gives the following system of eight linear algebraic equations for the coefficients of wave function (A1):

$$(E-E_g-\delta+\tfrac{1}{2}\hbar\omega)M+\frac{\gamma}{\lambda}X=0,$$

$$(E-E_g-\delta-\tfrac{1}{2}\hbar\omega)N+\frac{\gamma}{\lambda}Y=0,$$

$$\frac{\gamma}{\lambda}(l-1)M+(E-\delta+\alpha-\tfrac{3}{2}\beta+\tfrac{1}{2}\hbar\omega)A+2(l-1)\eta X=0,$$

$$\frac{\gamma}{2\lambda}M+(E+\delta+\alpha+\tfrac{1}{2}\beta+\tfrac{1}{2}\hbar\omega)B+\eta X-\delta D=0, \tag{A3}$$

$$-\gamma kM+(E+\alpha-\tfrac{1}{2}\beta+\tfrac{1}{2}\hbar\omega)C-2\lambda k\eta X+2\delta S=0,$$

$$\frac{\gamma}{\lambda}lN+(E+\delta+\alpha-\tfrac{1}{2}\beta-\tfrac{1}{2}\hbar\omega)S+2l\eta Y+\delta C=0,$$

$$\frac{\gamma}{2\lambda}N+(E-\delta+\alpha+\tfrac{3}{2}\beta-\tfrac{1}{2}\hbar\omega)T+\eta Y=0,$$

$$-\gamma kN+(E+\alpha+\tfrac{1}{2}\beta-\tfrac{1}{2}\hbar\omega)D-2\lambda k\eta Y-2\delta B=0,$$

where

$$X=A+2lB-\lambda kC,\quad Y=S+2(l+1)T-\lambda kD, \tag{A4}$$

$$\alpha=\frac{\hbar^2}{2m}(\gamma_1-2\gamma_2)\left(k^2+\frac{2l}{\lambda^2}\right),$$

$$\beta=\frac{\hbar^2}{2m}(\gamma_1-2\gamma_2)\frac{2}{\lambda^2},\quad \eta=\frac{\hbar^2}{2m}6\gamma_2\frac{1}{2\lambda^2}. \tag{A5}$$

To solve system (A3) for the electron states, one can neglect the terms with α, β, and η (i.e., let $\gamma_1=\gamma_2=0$). The presence of these terms in the equations for electrons gives a far too exact model. Then the electron spectrum splits into two branches:

$$E_{c\downarrow}^{c\uparrow}=\varepsilon_{c\downarrow}^{c\uparrow}+E_g+\delta\mp\tfrac{1}{2}\hbar\omega[1+O(\varepsilon_{c\downarrow}^{c\uparrow}/E_g)],$$

$$\frac{\varepsilon_{c\downarrow}^{c\uparrow}(\varepsilon_{c\downarrow}^{c\uparrow}+E_g)(\varepsilon_{c\downarrow}^{c\uparrow}+E_g+3\delta)}{\varepsilon_{c\downarrow}^{c\uparrow}+E_g+2\delta}=\gamma^2k^2+\frac{\gamma^2}{\lambda^2}\left(2l\mp1\mp\frac{\delta}{\varepsilon_{c\downarrow}^{c\uparrow}+E_g+2\delta}\right). \tag{A6}$$

Here the spectrum branch $c_\uparrow$ corresponds to the minus signs and the condition $N=0$ for the wave function coefficients and the branch $c_\downarrow$ corresponds to the plus signs and the condition $M=0$. The wave function coefficients derived from system (A3) are given by

$$M_{c\uparrow}=1,\quad N_{c\uparrow}=0,\quad A_{c\uparrow}=\frac{\gamma(l-1)/\lambda}{E-\delta},\quad T_{c\uparrow}=0,$$

$$B_{c\uparrow}=-\frac{\gamma E/(2\lambda)}{(E+2\delta)(E-\delta)},\quad C_{c\uparrow}=\frac{\gamma k(E+\delta)}{(E+2\delta)(E-\delta)},$$

$$S_{c\uparrow}=-\frac{\gamma k\delta}{(E+2\delta)(E-\delta)},\quad D_{c\uparrow}=-\frac{\gamma\delta/\lambda}{(E+2\delta)(E-\delta)}, \tag{A7}$$

$$M_{c\downarrow}=0,\quad N_{c\downarrow}=1,\quad A_{c\downarrow}=0,\quad T_{c\downarrow}=\frac{\gamma/(2\lambda)}{E-\delta},$$

$$B_{c\downarrow}=\frac{\gamma k\delta}{(E+2\delta)(E-\delta)},\quad C_{c\downarrow}=\frac{2l\gamma\delta/\lambda}{(E+2\delta)(E-\delta)},$$

$$S_{c\downarrow}=-\frac{l\gamma E/\lambda}{(E+2\delta)(E-\delta)},\quad D_{c\downarrow}=\frac{\gamma k(E+\delta)}{(E+2\delta)(E-\delta)}.$$

To solve Eqs. (A3) for the hole states, we have to introduce the coefficients

$$P=\frac{\lambda}{\gamma}(E-E_g-\delta)M\quad\text{and}\quad R=\frac{\lambda}{\gamma}(E-E_g-\delta)N \tag{A8}$$

instead of M and N. Finding the coefficients A, B, C, S, T, and D from the last six equations of system (A3) and substituting them into the first two equations gives the following system of two equations, which completely describes the hole states:

$$P+\frac{2(l-1)\theta P}{E_{-1,-\frac{3}{2},\frac{1}{2}}}+\frac{2l\theta E_{0,\frac{1}{2},-\frac{1}{2}}P-4l\lambda k\delta\theta R}{E_{1,\frac{1}{2},\frac{1}{2}}E_{0,\frac{1}{2},-\frac{1}{2}}-2\delta^2}$$

$$+\frac{2\lambda^2k^2\theta E_{1,-\frac{1}{2},-\frac{1}{2}}P+4l\lambda k\delta\theta R}{E_{1,-\frac{1}{2},-\frac{1}{2}}E_{0,-\frac{1}{2},\frac{1}{2}}-2\delta^2}=0,$$

$$R+\frac{2(l+1)\theta R}{E_{-1,\frac{3}{2},-\frac{1}{2}}}+\frac{2l\theta E_{0,-\frac{1}{2},\frac{1}{2}}R+2\lambda k\delta\theta P}{E_{1,-\frac{1}{2},-\frac{1}{2}}E_{0,-\frac{1}{2},\frac{1}{2}}-2\delta^2}$$

$$+\frac{2\lambda^2k^2\theta E_{1,\frac{1}{2},\frac{1}{2}}R-2\lambda k\delta\theta P}{E_{1,\frac{1}{2},\frac{1}{2}}E_{0,\frac{1}{2},-\frac{1}{2}}-2\delta^2}=0, \tag{A9}$$

where

$$E_{n_\delta,n_\beta,n_\omega}=E+n_\delta\delta+\alpha+n_\beta\beta+n_\omega\hbar\omega, \tag{A10}$$

$$\theta=\frac{1}{4}\left(\frac{m}{m_l}-\frac{m}{m_h}\right)\hbar\omega, \tag{A11}$$

$$\frac{m}{m_l}=\frac{2m\gamma^2}{\hbar^2(E_g+\delta-E)}+\frac{m}{m_h}+6\gamma_2 \quad \text{and} \quad \frac{m}{m_h}=\gamma_1-2\gamma_2. \tag{A12}$$

Here m_h coincides with the heavy hole mass, and m_l with the light hole mass, in the case of zero constant of spin-orbit interaction. Similarly, the electron mass is given by

$$\frac{m}{m_c}=\frac{2m\gamma^2}{\hbar^2E_g}\frac{E_g+2\delta}{E_g+3\delta}. \tag{A13}$$

The system (A9) can be easily solved under condition $\gamma_1=\gamma_2=0$ used above to obtain the electron spectrum (A6). This approximation helps to separate the heavy hole branches from the hole spectra. The mixing between the states of heavy and light holes (and, respectively, that between states of heavy and spin-orbit split off holes) is low due to a certain difference in the masses $m_l \ll m_h$. This mixing is described below in detail. Now let us write down the hole spectra in the approximation $\gamma_j=0 (j=1,2)$:

$$E_{lh\uparrow\downarrow}^{so\uparrow\downarrow}=-\tfrac{1}{2}(\delta+\varepsilon^{\uparrow}_{\downarrow})\mp d_{so}^{lh}\sqrt{2\delta^2+\tfrac{1}{4}(\delta-\varepsilon^{\uparrow}_{\downarrow})^2+c^{\uparrow}_{\downarrow}\tfrac{1}{2}\delta\hbar\omega_l}$$

$$-c^{\uparrow}_{\downarrow}\tfrac{1}{2}\hbar\omega[1+O(\varepsilon^{\uparrow}_{\downarrow}/E_g)], \tag{A14}$$

$$\varepsilon^{\uparrow}_{\downarrow}=\hbar\omega_l(l\mp\tfrac{1}{2})+\frac{\hbar^2k^2}{2m_l}, \quad c^{\uparrow}_{\downarrow}=\pm1, \quad d_{so}^{lh}=\pm1.$$

Here $\hbar\omega_j=\hbar\omega m/m_j$ with $j=\{l,h,c\}$; $c^{\uparrow}_{\downarrow}=+1$ for the $lh_\uparrow$ and $so_\uparrow$ branches of the spectrum, and $c^{\uparrow}_{\downarrow}=-1$ for the $lh_\downarrow$ and $so_\downarrow$ branches; $d_{so}^{lh}=+1$ for $lh_\uparrow$ and $lh_\downarrow$, and $d_{so}^{lh}=-1$ for $so_\uparrow$ and $so_\downarrow$; the minus sign in $E_{lh\uparrow\downarrow}^{so\uparrow\downarrow}$ corresponds to $so_\uparrow$ and $so_\downarrow$, and the plus sign to $lh_\uparrow$ and $lh_\downarrow$; the minus sign in $\varepsilon^{\uparrow}_{\downarrow}$ corresponds to $lh_\uparrow$ and $so_\uparrow$, and the plus sign to $lh_\downarrow$ and $so_\downarrow$. The wave function coefficients are similar to those obtained for electrons (A7). Indeed, the $lh_\uparrow$ and $so_\uparrow$ branches correspond to the condition $R=0$ (and therefore, $N=0$) imposed on the wave function coefficients, and $lh_\downarrow$ and $so_\downarrow$ to $P=0$ (and therefore, $M=0$). We do not write down the wave function coefficients because of the complexity of the corresponding expressions.

For the heavy hole states, $N=0$ and $M=0$ simultaneously in the $\gamma_j=0$ approximation. Furthermore, the expression $M=N=0$ is valid for heavy hole states when γ_j terms are taken into account in the absence of magnetic field.[12] In this case, the spectrum of heavy holes is given by $E_h=\delta-\hbar^2k^2/2m_h$.[12] However, the condition $M=N=0$ is broken in the presence of magnetic field. In this case the heavy hole spectrum can be written in the form $E=\delta-\alpha+\varepsilon$ where $|\varepsilon|\ll\delta$ by analogy with the result obtained in the absence of magnetic field.[12] Supposing $|\varepsilon|\ll\delta$ helps to ignore the spin-orbit split off holes. Substitution $E=\delta-\alpha+\varepsilon$ into system (A9) gives

$$\varepsilon^4+\tfrac{8}{3}(\lambda^2k^2+2l)\theta\varepsilon^3$$

$$+[\tfrac{16}{9}((\lambda^2k^2+2l)^2-\tfrac{9}{4})\theta^2-6\theta\beta-\tfrac{5}{2}\beta^2]\varepsilon^2$$

$$-[\tfrac{16}{3}(\lambda^2k^2+2l)\theta^2\beta+6(\lambda^2k^2+\tfrac{2}{3}l)\theta\beta^2]\varepsilon$$

$$-[4((\lambda^2k^2+l)^2-l^2-\tfrac{1}{4})\theta^2\beta^2+\tfrac{3}{2}\theta\beta^3+\tfrac{9}{16}\beta^4]=0. \tag{A15}$$

Here we omit the terms $\pm\frac{1}{2}\hbar\omega$ in system (A9) to simplify Eq. (A15). These terms can be added directly to the spectra obtained from (A15). Two small parameters can be introduced in Eq. (A15). One of these, $(\lambda k)^{-2}$, is much less than unity in the case $a^2\ll\lambda^2$, and the other, β/θ, does so by virtue of the condition $m_l\ll m_h$. The spectra of heavy and light holes can be derived from Eq. (A15) with the use of perturbation theory based on expansion in the small parameter $(\lambda k)^{-2}$. The light hole spectrum series

$$E_{\mathrm{lh}\downarrow}^{\mathrm{lh}\uparrow}=\delta-\alpha+\varepsilon_{\mathrm{lh}\downarrow}^{\mathrm{lh}\uparrow}\mp\tfrac{1}{2}\hbar\omega[1+O(\varepsilon_{\mathrm{lh}\downarrow}^{\mathrm{lh}\uparrow}/E_g)],$$

$$\varepsilon_{\mathrm{lh}\downarrow}^{\mathrm{lh}\uparrow}=-\frac{4}{3}\theta\left(\lambda^2k^2+2l\mp\frac{3}{2}\mp\frac{3\beta}{8\theta}\right) \tag{A16}$$

demonstrates that the mixing of the heavy hole states to the light hole states is negligible in the common cases. This expression is equal to (A14) in the limits $\beta\ll\theta$ and $|E-\delta|\ll\delta$. The heavy hole spectrum series

$$E_{hh\downarrow}^{hh\uparrow}=\delta-\alpha+\varepsilon_{hh\downarrow}^{hh\uparrow}\mp\tfrac{1}{2}\hbar\omega[1+O(\varepsilon_{hh\downarrow}^{hh\uparrow}/E_g)],$$

$$\varepsilon_{hh\downarrow}^{hh\uparrow}=\pm\frac{3}{2}\beta\Bigg[1-(l\mp1)(\lambda k)^{-2}$$

$$+\left(\frac{3}{2}(l\mp1)^2\pm\frac{3\beta}{4\theta}(l\mp1)\right)(\lambda k)^{-4}\Bigg] \tag{A17}$$

shows even less mixing than that of the light holes (A16). The heavy hole wave function coefficients are given by

$$M_{hh\uparrow}=-\frac{2\gamma k}{E-E_g-\delta},\quad N_{hh\uparrow}=\frac{\gamma/\lambda}{E-E_g-\delta},$$

$$A_{hh\uparrow}=\frac{8\theta}{3\beta}(\lambda k)^3,\quad B_{hh\uparrow}=-\frac{2\theta}{3\beta}\lambda k,\quad C_{hh\uparrow}=\frac{8\theta}{3\beta}(\lambda k)^2,$$

$$S_{hh\uparrow}=-\frac{4\theta}{3\beta}(\lambda k)^2,\quad T_{hh\uparrow}=\frac{\theta}{3\beta},\quad D_{hh\uparrow}=-\frac{4\theta}{3\beta}\lambda k,$$

$$M_{hh\downarrow}=-\frac{l(l+1)\gamma/\lambda}{E-E_g-\delta},\quad N_{hh\downarrow}=\frac{(l+1)\gamma k}{E-E_g-\delta},\quad \text{(A18)}$$

$$A_{hh\downarrow}=-\frac{2\theta}{3\beta}(l-1)l(l+1),\quad B_{hh\downarrow}=\frac{2\theta}{3\beta}(l+1)(\lambda k)^2,$$

$$S_{hh\downarrow}=-\frac{2\theta}{3\beta}l(l+1)\lambda k,\quad T_{hh\downarrow}=\frac{2\theta}{3\beta}(\lambda k)^3,$$

$$C_{hh\downarrow}=\frac{4\theta}{3\beta}l(l+1)\lambda k,\quad D_{hh\downarrow}=\frac{4\theta}{3\beta}(l+1)(\lambda k)^2.$$

It can be seen from the analysis given above that the hh and lh states do not mix in the limit $H\to 0$. This limit is equivalent to the limit $k_{x,y}\to 0$ in the absence of magnetic field (see above), where the hh and lh components are known to be decoupled.[20]

The lowest Landau levels require special attention. Some components of the wave function (A1) disappear when the Landau level index takes the values $l=-1,0,1$. The wave function is identically zero at $l<-1$. Investigating each of three cases $l=-1,0,1$ separately shows that only the $hh_\downarrow$ branch exists for $l=-1$, only $hh_\downarrow$, $lh_\downarrow$, $so_\downarrow$, and $c_\downarrow$ branches for $l=0$, and all branches but $hh_\uparrow$ for $l=1$.[19] In other words, different branches of the spectrum have different minimal Landau level indices:

$$\begin{aligned} hh_\downarrow:&\quad l\geqslant -1,\\ lh_\downarrow, so_\downarrow, c_\downarrow:&\quad l\geqslant 0,\\ lh_\uparrow, so_\uparrow, c_\uparrow:&\quad l\geqslant 1,\\ hh_\uparrow:&\quad l\geqslant 2. \end{aligned}\qquad \text{(A19)}$$

This implies that the $l=-1$ level is a purely $hh_\downarrow$ state.[22] Indeed, one can see from (A17) that $E_{hh\downarrow}=\delta-\alpha-\frac{3}{2}\beta$ for $l=-1$, i.e., the lh states are not mixed to the level $hh_\downarrow, l=-1$.

The wave function of a carrier in the quantum well (6) is given by (7), (8), and (A1). The electron wave function is a superposition of $c_\uparrow$ and $c_\downarrow$ states. The dispersion equation can be obtained from boundary conditions (9). For the electron states, these boundary conditions require only continuity at the heteroboundaries for the components Ψ_s and Ψ_{pz} of the wave function. Substituting the electron wave function $\Psi=C_{c\uparrow}\Psi_{c\uparrow}+C_{c\downarrow}\Psi_{c\downarrow}$ into these boundary conditions gives the following dispersion equation for electrons:

$$\left(k_{c\uparrow}\tan\frac{k_{c\uparrow}a}{2}-G\kappa_{c\uparrow}\right)\left(k_{c\downarrow}\cot\frac{k_{c\downarrow}a}{2}+G\kappa_{c\downarrow}\right)=-\frac{2l\delta^2(1-\tilde{G})}{\lambda^2(E_g+2\delta+\varepsilon_c)^2}.\qquad \text{(A20)}$$

Here the chosen symmetry of wave functions $\Psi_{c\uparrow}$ and $\Psi_{c\downarrow}$ corresponds to the sign plus in (7), κ_c is the modulus of the z component of the electron wave vector in the barrier region, and G and $\tilde{G}$ are the coefficients defined by

$$G=\frac{(E_g+\varepsilon_c)(E_g+3\delta+\varepsilon_c)(E_g+V_v+2\tilde{\delta}+\varepsilon_c)}{(E_g+V_v+\varepsilon_c)(E_g+V_v+3\tilde{\delta}+\varepsilon_c)(E_g+2\delta+\varepsilon_c)},$$

$$\tilde{G}=\frac{\tilde{\delta}}{\delta}\frac{E_g+2\delta+\varepsilon_c}{E_g+V_v+2\tilde{\delta}+\varepsilon_c}G.\qquad \text{(A21)}$$

The dispersion equation splits into two parts if the Landau level number l is small or the coefficient $\tilde{G}$ is close to unity. The last condition is usually fulfilled in semiconductors with similar band structures. Choosing the opposite wave function symmetry [i.e., the sign minus in the wave function (7)] gives the same dispersion equation (A20) with interchanged indices $c_\uparrow$ and $c_\downarrow$. Finally, the electron spectrum is approximately given by the following two separated dispersion equations:

$$k_{c\uparrow\downarrow}\tan\frac{k_{c\uparrow\downarrow}a}{2}=G\kappa_{c\uparrow\downarrow}\quad\text{and}\quad k_{c\uparrow\downarrow}\cot\frac{k_{c\uparrow\downarrow}a}{2}=-G\kappa_{c\uparrow\downarrow}.\qquad \text{(A22)}$$

They are similar to the dispersion equations for heavy holes

$$k_{hh\uparrow\downarrow}\tan\frac{k_{hh\uparrow\downarrow}a}{2}=\kappa_{hh\uparrow\downarrow}\quad\text{and}\quad k_{hh\uparrow\downarrow}\cot\frac{k_{hh\uparrow\downarrow}a}{2}=-\kappa_{hh\uparrow\downarrow}\qquad \text{(A23)}$$

obtained in the approximation of unmixed light and heavy hole states (i.e., the quantum mechanical spectrum of a particle in a rectangular quantum well).

[1] R. Dornhaus *et al.*, Phys. Rev. Lett. **37**, 710 (1976).
[2] B. L. Gelmont, Zh. Eksp. Teor. Fiz. **75**, 536 (1978); [Sov. Phys. JETP **48**, 268 (1978)].
[3] M. Takeshima, Phys. Rev. B **28**, 2039 (1983).
[4] A. D. Andreev and G. G. Zegrya, Zh. Eksp. Teor. Fiz. **105**, 1005 (1994); [Sov. Phys. JETP **78**, 539 (1994)].
[5] M. Potemski *et al.*, Phys. Rev. Lett. **66**, 2239 (1991).
[6] I. Maran *et al.*, Semicond. Sci. Technol. **9**, 700 (1994).

[7] E. Tsitsishvili and Y. Levinson, Phys. Rev. B **56**, 6921 (1997).
[8] W. W. Lui *et al.*, Phys. Rev. B **48**, 8814 (1993).
[9] N. K. Dutta, J. Appl. Phys. **54**, 1236 (1983).
[10] G. G. Zegrya and V. A. Kharchenko, Zh. Eksp. Teor. Fiz. **101**, 327 (1992); [Sov. Phys. JETP **74**, 173 (1992)].
[11] M. I. Dyakonov and V. Yu. Kachorovskii, Phys. Rev. B **49**, 17 130 (1994).
[12] A. S. Polkovnikov and G. G. Zegrya, Phys. Rev. B **58**, 4039 (1998).
[13] E. O. Kane, J. Phys. Chem. Solids **1**, 249 (1957).
[14] P. C. Sercel and K. J. Vahala, Phys. Rev. B **42**, 3690 (1990).
[15] R. A. Suris, Fiz. Tekh. Poluprovodn. (St. Petersburg) **20**, 2008 (1986); [Sov. Phys. Semicond. **20**, 1258 (1986)].
[16] M. G. Burt, J. Phys.: Condens. Matter **4**, 6651 (1992).
[17] B. A. Foreman, Phys. Rev. B **49**, 1757 (1994).
[18] G. L. Bir and G. E. Pikus, *Symmetry and Strain-Induced Effects in Semiconductors* (Wiley, New York, 1974).
[19] G. Y. Wu, T. C. McGill, C. Mailhiot, and D. L. Smith, Phys. Rev. B **39**, 6060 (1989).
[20] F. Ancilotto, A. Fasolino, and J. C. Maan, Phys. Rev. B **38**, 1788 (1988).
[21] I. S. Gradshteyn and I. M. Ryzhik, *Table of Integrals, Series, and Products* (Academic, New York, 1994).
[22] S. L. Wong, R. J. Warburton, R. J. Nicholas, N. J. Mason, and P. J. Walker, Phys. Rev. B **49**, 11 210 (1994).